Article

The gem-Dialkyl Effect in Diphosphine Ligands: Synthesis, Coordination Behavior and Application in Pd-catalyzed Hydroformylation

Dillon W. P. Tay, James D. Nobbs, Charles Romain, Andrew J. P. White, Srinivasulu Aitipamula, Martin van Meurs, and George J.P. Britovsek

ACS Catal., **Just Accepted Manuscript** • DOI: 10.1021/acscatal.9b03007 • Publication Date (Web): 03 Dec 2019

The *gem*-Dialkyl Effect in Diphosphine Ligands: Synthesis, Coordination Behavior and Application in Pd-catalyzed Hydroformylation

Dillon W. P. Tay, James D. Nobbs,† Charles Romain, Andrew J. P. White, Srinivasulu Aitipamula,† Martin van Meurs,† George J. P. Britovsek.*

Department of Chemistry, Imperial College London, Molecular Sciences Research Hub, White City Campus, 80 Wood Lane, W12 0BZ, United Kingdom. †Institute of Chemical and Engineering Sciences, Agency for Science, Technology & Research, Jurong Island, Singapore 627833.

ABSTRACT: A series of palladium complexes with C_3-bridged bidentate bis(diphenylphosphino)propane ligands with substituents of varying steric bulk at the central carbon have been synthesized. The size of the gem-dialkyl substituents affects the C–C–C bond angles within the ligands and consequently the P–M–P ligand bite angles. A combination of solid state XRD and DFT studies has shown that an increase in substituent size results in a distortion of the 6-membered metal-ligand chair conformation towards a boat conformation, in order to avoid bond angle strain. The influence of the gem-dialkyl effect on the catalytic performance of the complexes in palladium-catalysed hydroformylation of 1-octene has been investigated. While hydroformylation activity to nonanal decreases with increasing size of the gem-dialkyl substituents, a change in chemo-selectivity towards nonanol via reductive hydroformylation is observed.

KEYWORDS: Thorpe-Ingold, hydroformylation, gem-dialkyl, chelate, bidentate, diphosphine

1. INTRODUCTION

Advancements in transition metal co-ordination chemistry and in understanding organometallic reaction mechanisms have led to continual improvements in homogeneous catalyst development.[1] Despite the importance typically placed on the identity of the transition metal in catalyst design, the characteristics of the ancillary ligand can be critical for catalyst stability, controlling reaction rates and determining chemo- and regioselectivity.[2] Ligand σ-donor and π-acceptor properties influence the electronic environment at the metal center, while ligand structure and co-ordination geometry impose steric constraints that affect the spatial environment. For monodentate phosphines, these steric and electronic parameters are classically quantified via the Tolman electronic parameter, χ, and ligand cone angle, θ.[3-5] In the case of bidentate ligands, these parameters are insufficient to account for the additional nuances introduced by ligand backbone structure and bidentate chelation.[6-7] In order to capture this, Casey and Whiteker introduced the concept of natural bite angle, β_n,[8] which gives an indication of the preferred chelation angle determined by ligand backbone rigidity in bidentate phosphines.[8] This natural bite angle β_n can provide a quantitative measure of the relationship between ligand backbone structure and catalytic performance. It has been used to show how ligand bite angles can influence the catalytic cycle by stabilizing (or destabilizing) initial or final reaction intermediates and transition states,[9] thereby effecting significant changes in catalyst activity and selectivity.[10]

A straightforward way to modify ligand bite angle is to adjust the length of the ligand backbone, since longer backbones typically result in larger bite angles, but with increased flexibility.[7] Conversely, a rigid ligand backbone such as 1,2-phenylene can be employed to enforce a certain bite angle.[11] A less direct and more subtle modification, which has been investigated here, is to manipulate the bite angle through *gem*-dialkyl substitution at the ligand backbone (see Figure 1).

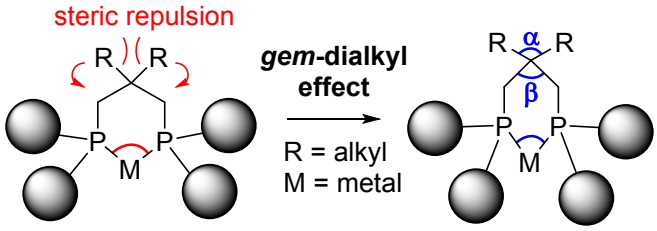

Figure 1. The *gem*-dialkyl effect in diphosphine ligands.

Steric repulsion between geminal alkyl groups (R) can simultaneously widen the R-C-R α bond angle and compress the C-C-C β bond angle, thereby indirectly altering the P-M-P bite angle and the steric environment around the metal centre. An electronic effect from the geminal dialkyl groups on the phosphine donors is also possible, but is expected to be relatively minor compared to the steric effects, due to the remoteness and weak electron-donating properties of the alkyl groups. A *gem*-dialkyl effect in diphosphine ligands has been observed previously, for example to modify reaction rates,[12-13] regioselectivity[14] or substitution behavior.[15]

In organic synthesis, the *gem*-dialkyl effect, better known as the Thorpe-Ingold effect, has been known for over a century to accelerate cyclization reactions by favoring reactive rotamers and stabilizing ring structures.[16-18] In contrast, there is comparatively little insight into its role and impact on ligands in coordination chemistry and catalysis. As a well-established phenomenon in organic synthesis, previous studies on the *gem*-dialkyl effect can provide a basis for predicting how ligand structure and subsequent co-ordination bahaviour may be influenced. However, extrapolating to how this might affect catalytic performance remains non-trivial.

In this paper, we report the synthesis and characterization of a series of bidentate bis(diphenylphosphine)propane ligands **L1-L4** with different geminal dialkyl groups at the central carbon of the ligand backbone (Chart 1). A detailed conformational analysis of the ligand binding modes, effects on coordination environment and space around the metal center has been carried out using structural and computational techniques. The diphosphine ligands have been applied in the hydroformylation of 1-alkenes, arguably one of the most important applications in homogeneous catalysis.[19-20] In the case of Pd-catalyzed hydroformylation of 1-octene, we show that *gem*-dialkyl substitution reduces hydroformylation activity and alters chemoselectivity to favor reductive hydroformylation. Reductive hydroformylation, the direct conversion of alkenes to alcohols using a combined hydroformylation/hydrogenation protocol, has seen renewed interest in recent years.[21]

2. RESULTS AND DISCUSSION

Synthesis and Characterisation

The synthesis of the ligand series was envisioned to proceed via S_N2 nucleophilic substitution of the corresponding electrophilic precursors with lithium diphenyl phosphide, as shown in Figure 2.

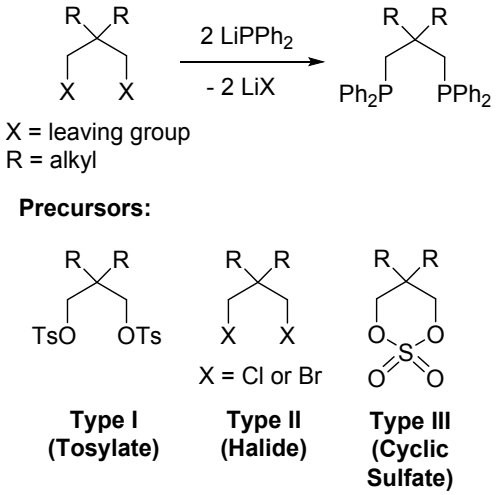

Figure 2. General synthetic pathway ligands **L2-L4**.

Three classes of electrophiles were investigated: tosylates (**Type I**), halides (**Type II**) and cyclic sulfates (**Type III**). These functionalities were selected for their weak conjugate basicity implying good leaving group ability, and in the case of tosylates and cyclic sulfates, for their ability to activate 1,3-diols toward nucleophilic substitution.

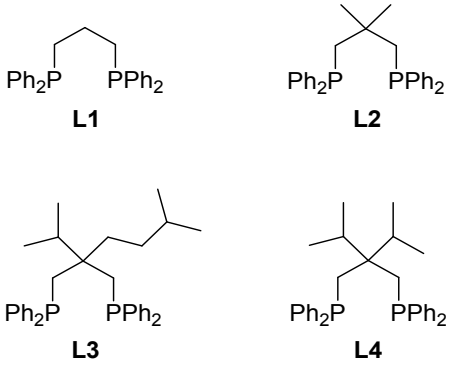

Chart 1. Series of Bidentate Bis(diphenylphosphino)propane Ligands **L1-L4.**

Ligand Precursors

Hydrogenation followed by a cross-Cannizzaro reaction with formaldehyde[22] yielded asymmetric *iso*-propyl/*iso*-pentyl diol from commercially available 2-isopropyl-5-methyl-2-hexanal. This was then used to make precursors **1-3** (see Figure 3).

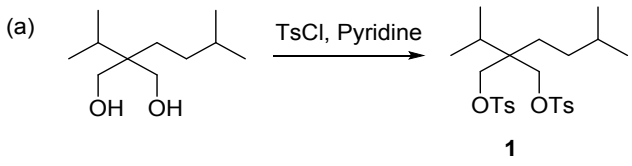

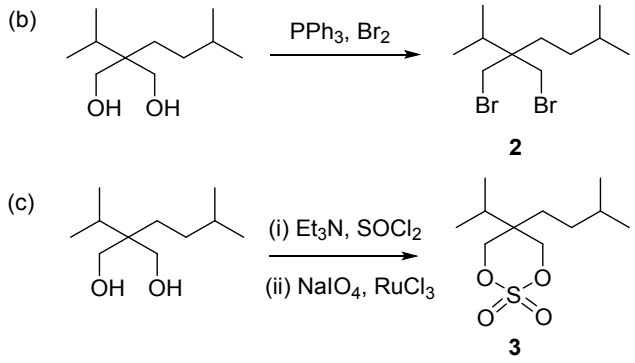

Figure 3. (a) Synthesis of tosylate **1**. (b) Synthesis of bromo-analog **2**. (c) Synthesis of cyclic sulfate **3**.

Both tosylate **1** and cyclic sulfate **3** were prepared via known procedures,[23-25] while bromo-analog **2** was prepared via the Appel reaction.

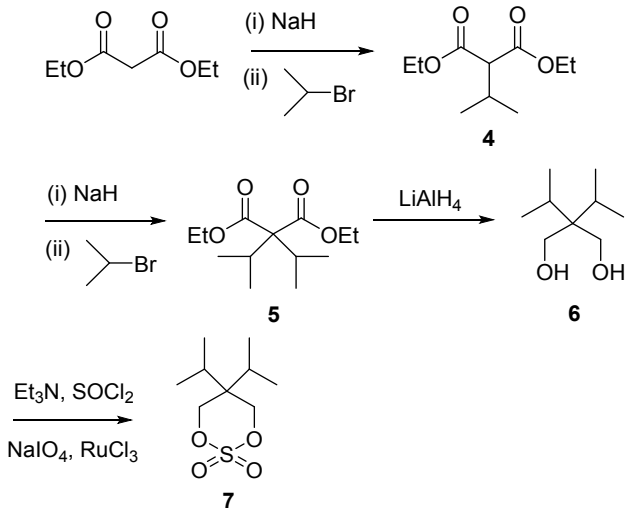

Figure 4. Synthesis of di-*iso*-propyl cyclic sulfate **7**.

The synthesis of precursor **7** required a different approach (see Figure 4). The synthesis of di-*iso*-propyl malonate **5** required excess isopropyl bromide to go to completion. This was attributed to deprotonated malonate **4** acting as a base (E2 mechanism) instead of a nucleophile (S_N2 mechanism) on isopropyl bromide to give propene because of its sterically hindered tertiary carbanion. Despite this, 99% conversion to di-*iso*-propyl substituted malonate **5** was achieved through repeated additions of isopropyl bromide in excess. Subsequent reduction of malonate **5** with $LiAlH_4$ yielded diol **6** that was then converted to di-*iso*-propyl cyclic sulfate **7** using the methodology employed previously for *iso*-propyl/*iso*-pentyl analog **3**.

Diphosphine Ligand Synthesis

The synthesis of ligands **L2-L4** was accomplished via S_N2 substitution of the ligand precursors with *in-situ* generated lithium diphenyl phosphide and the results are summarized in Table 1.

Table 1. Synthesis of *gem*-Dialkyl Substituted Bidentate Bis(diphenylphosphino)propane Ligands.

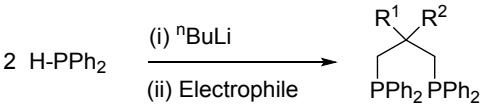

L1: $R^1 = R^2 = H$ **L3**: $R^1 = i$Pr, $R^2 = i$Pent
L2: $R^1 = R^2 = Me$ **L4**: $R^1 = R^2 = i$Pr

L	Electrophile	R^1	R^2	Time / h	Yield* / %
L2	Type I	Me	Me	24	0
L2	Type II (Cl)	Me	Me	24	96
L3	Type II (Br)	*i*Pr	*i*Pent	72	16
L3	Type III	*i*Pr	*i*Pent	96	14
L4	Type III	*i*Pr	*i*Pr	168	11

Conditions: H-PPh_2 (2.1 eq), electrophile (1 eq), ^{n}BuLi (2.1 eq), THF, 65 °C. *Isolated yields.

The $^{31}P\{^1H\}$ NMR spectrum of the reaction mixture from the synthesis of **L2** from **Type I** tosylate precursor showed a major phosphorus product (ca. 48%) as a singlet at -15.0 ppm, which suggests Ph_2P-PPh_2 (literature value[26] = -15.2 ppm). No desired product **L2** was observed, and 22% of the starting tosylate was recovered. This is consistent with an earlier report by Eberhard, who demonstrated that undecorated C_3-bridged di-tosylates could be used to prepare bidentate diphosphine ligands through treatment with lithium phosphides. However, upon *gem*-dimethylation of the central carbon, P-P bonded species were obtained as major by-products.[27] Earlier work by Harris and Pretzer on the synthesis of P-P diphosphines from alkyl halides reported a proposed mechanism for the formation of these species.[28] In order to avoid these side reactions, subsequent synthetic efforts were focused on **Type III** cyclic sulfate precursors that did not possess the halide groups that were implicated in their formation.

The synthesis of asymmetric *iso*-propyl/*iso*-pentyl ligand **L3** from **Type III** cyclic sulfate precursor gave a reaction mixture that had a $^{31}P\{^1H\}$ NMR spectrum containing **L3** as a singlet at -25.3 ppm (ca. 60%) with a single major by-product as a singlet at -16.3 ppm (ca. 36%). The mixture was protected with BH_3, separated via column chromatography, and deprotected with refluxing EtOH to give **L3** in modest yield (14%).[29] A similar procedure yielded the di-*iso*-propyl ligand **L4** in modest yield (11%). Subsequent modifications attempting to improve yield using $LiPPh_2$ with **Type II (Br)** precursor resulted in a product mixture with similar ^{31}P signals. This suggests that the identity of the leaving group does not play a significant role in the occurring side reaction, and

that it may be a problem with the synthetic strategy in general. A possible alternative to circumvent this could involve an Umpolung-type reversal of polarities, generating di-Grignards from 1,3-dihalides as the nucleophile to attack chlorophosphine electrophiles instead.[30]

Palladium Complexes

The ligands **L2**-**L4** were combined with [Pd(COD)Cl_2] to give the corresponding [Pd(**L**)Cl_2] complexes in excellent yield (see Figure 5 and Supporting Information for details). Single crystals suitable for XRD analysis were grown either via layering of pentane on a DCM solution of the complex or via slow diffusion of cyclohexane into a DCM solution of the complex (Figure 6).

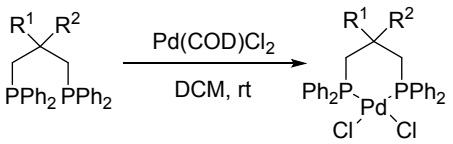

$R^1 = R^2$ = Me, Pd(**L2**)Cl_2: 97% yield
R^1 = *i*Pr, R^2 = *i*Pent, Pd(**L3**)Cl_2: 96% yield
$R^1 = R^2$ = *i*Pr, Pd(**L4**)Cl_2: 99% yield

Figure 5. Synthesis of Pd(**L**)Cl_2 complexes.

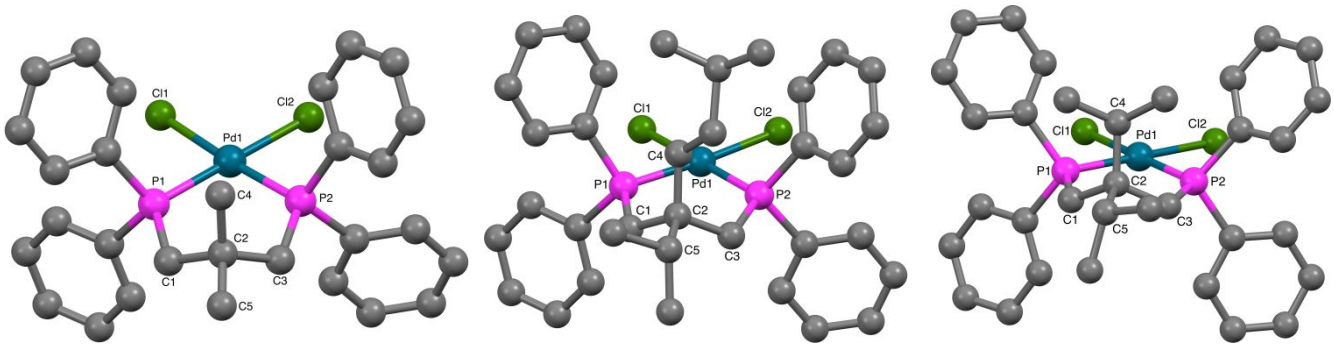

Figure 6. Crystal structures of Pd(**L**)Cl_2 complexes of **L2** (left), **L3** (middle) and **L4** (right) with displacement ellipsoids shown at 50% probability. Hydrogen atoms omitted, and only selected atoms labelled for clarity.

Table 2. Selected Bond Lengths (Å) and Angles (°) of Pd(L)Cl_2.[a]

	Pd(**L1**)Cl_2	Pd(**L2**)Cl_2	Pd(**L3**)Cl_2	Pd(**L4**)Cl_2
C^4-C^2-C^5 (α)	-	109.5 (3)	109.5 (3)	111.74 (19)
C^1-C^2-C^3 (β)	117.0 (5)	110.1 (3)	108.2 (3)	107.27 (19)
P^1-Pd^1-P^2	90.58 (5)	95.84 (3)	96.29 (4)	94.69 (2)
Cl^1-Pd^1-Cl^2	90.78 (5)	91.59 (3)	91.85 (4)	90.95 (3)
P^2-Pd^1-Cl^2	91.10 (5)	84.49 (3)	86.37 (4)	86.66 (2)
P^1-Pd^1-Cl^1	87.74 (5)	88.09 (3)	85.59 (4)	87.69 (3)
P^1-Pd^1	2.249 (2)	2.2371 (9)	2.2452 (11)	2.2386 (7)
P^2-Pd^1	2.244 (1)	2.2423 (9)	2.2449 (11)	2.2433 (6)
Pd^1-Cl^2	2.351 (1)	2.3391 (9)	2.3480 (10)	2.3586 (7)
Pd^1-Cl^1	2.358 (2)	2.3570 (9)	2.3381 (12)	2.3435 (7)

[a] Values for [Pd(**L1**)Cl_2] taken from literature.[31]

Comparison of β angles in the solid state structures of [Pd(**L**)Cl2] across the series shows a decreasing trend going from 117° (**L1**) to 107° (**L4**) (see Table 2). From **L3** to **L4**, the *gem*-dialkyl effect of concurrent α angle expansion and β angle compression is clearly noticeable. There is a 2° decrease between **L2** and **L3** as the α angle remains essentially the same at the ideal tetrahedral value of 109.5°. It is noteworthy that despite a lack of change in α angle between **L2** and **L3**, the *gem*-dialkyl effect still shows a β angle compression. This bond angle modification is due to a distortion in the 6-membered chelate ring comprising of the C_3 backbone, both P donor atoms and the Pd metal center. The original chair conformation adopted in the case of **L1** and **L2** distorts towards a half-chair in **L3**, with the Pd metal atom moving upwards toward planarity with the P donor atoms, while maintaining the square planar geometry expected of a Pd(II) d^8 complex.

There is an increase in P-Pd-P ligand bite angle from 91° (**L1**) to 95-96° (**L2**-**L4**). It is clear from this study that this parameter alone is not sufficient to describe the ligand system. Due to distortions in the 6-membered chelate ring, the relationship between *gem*-dialkyl group size and ligand bite angle is complicated. The perturbation of the P-Pd-P bite angle is accommodated without altering the Cl-Pd-Cl bond angle, which remains constant at 90-91° across the series. Instead, a distortion

of the square planar geometry of the Pd(II) complex occurs, which is shown in Figure 7 as a twisting of the chlorides out of the P-Pd-P plane.

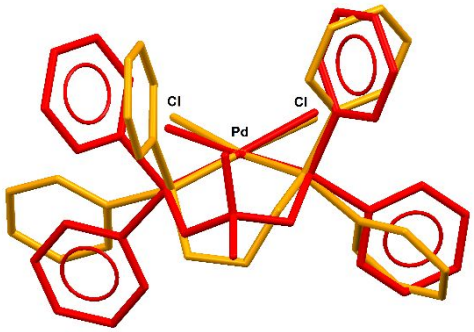

Figure 7. Overlaid crystal structures of Pd(**L1**)Cl_2 (orange) and Pd(**L2**)Cl_2 (red).

There are also subtle changes in the overall spatial orientation of the ligand that influence the coordination sphere around the metal center. Classical methods of quantifying ligand steric bulk such as the Tolman cone angle[3] are not sufficient to probe these nuances since it measures the substituents directly connected to the P donor atom. The *gem*-dialkyl effect acts as an indirect modification via the ligand backbone to influence the overall structure of the complex without modifying the substituents directly attached to the P donor atoms. Falivene and co-workers have introduced a more comprehensive computational tool to probe the coordination sphere around a metal center, with a parameter termed ligand buried volume (%V_Bur).[32] The percentage ligand buried volume is defined as the amount of space occupied by the ligand of interest in a sphere of a specified radius around a given coordination center, which in our case, is the Pd metal atom. Comparison of the calculated %V_Bur of the diphenyl ligand series shows a trend of increasing steric congestion from **L1** (38.9%), **L2** (41.1%), **L3** (41.8%) and finally **L4** (42.2%) in a sphere of radius 5 Å around the Pd center (see Figure 8).

Computational DFT Study

All theoretical calculations were carried out with Gaussian 16.[33] In addition to the [Pd(L)Cl_2] complexes of the four synthesized bis(diphenylphosphino)propane ligands R = H (**L1**), Me (**L2**), ^{i}Pr/^{i}Pent (**L3**) and ^{i}Pr (**L4**), the diethyl (**L^{Et}**) and di(tert.-butyl) (**L^{tBu}**) ligands have been calculated for comparison (see Figure 8). Final geometry optimizations were carried out with hybrid functional B3LYP[34-35] in combination with triple-ζ DEF2TZVPP[36-37] basis set for C, H, O and P atoms and the Stuttgart-Dresden (SDD) effective core potential (ECP) with the corresponding basis set for Pd. All calculations were performed at 298.15 K and at 423.15 K with Grimme dispersion correction[38] and Becke-Johnson damping.[39-40]

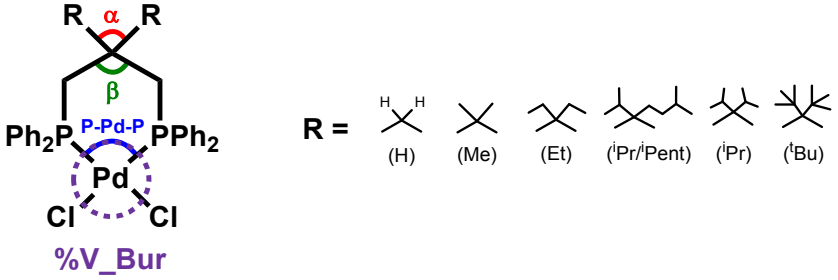

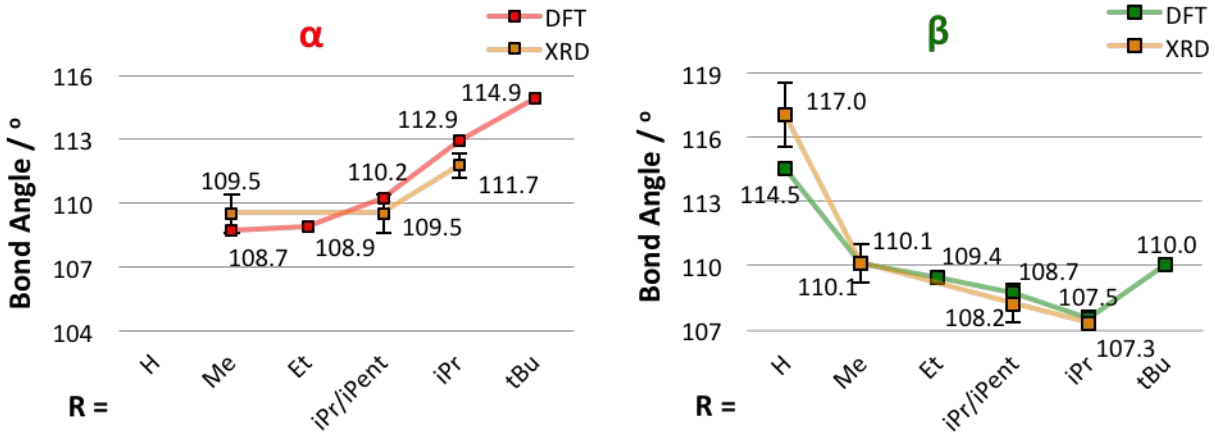

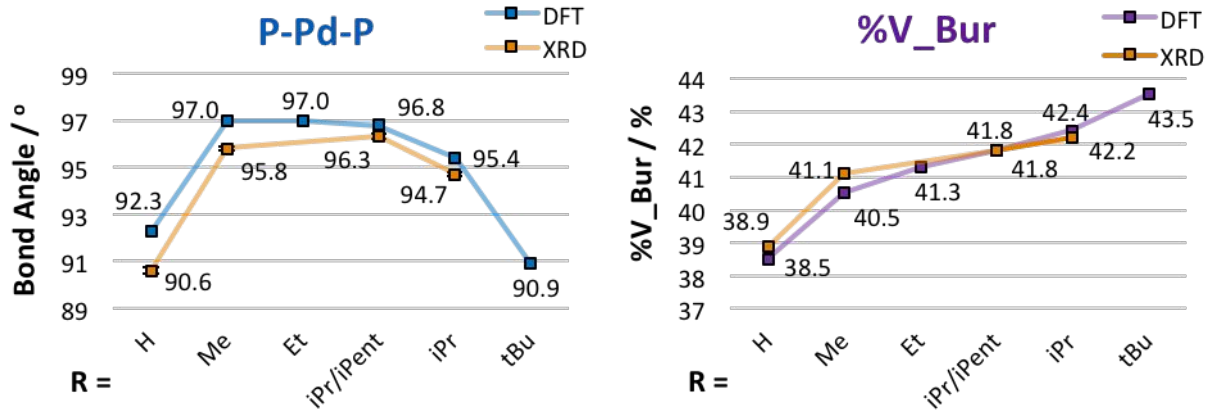

Figure 8. Graphs of Pd(**L**)Cl_2 parameters with error bars at 99.7% confidence. (i) *Top Left*: ∠ angle vs. R group (ii) *Top Right*: ∠ angle vs. R group (iii) *Bottom Left*: P-Pd-P angle vs. R group (iv) *Bottom Right*: %V_Bur vs. R group.

The calculated α angle increases with increasing steric bulk of the geminal R groups, from 109° in the dimethyl ligand (**L2**) to 115° for the di-*tert*-butyl ligand. Conversely, the β angles decrease from 115° for the plain ligand (**L1**, where R = H) to 107° for the di-*iso*-propyl ligand (**L4**). This simultaneous α angle expansion and β angle compression follows what is expected of the *gem*-dialkyl effect. Interestingly, the calculated β angle appears to increase to 110° for the bulkiest di-*tert*-butyl ligand (**L^{tBu}**). Upon closer inspection of the structures, it appears that the steric repulsion of the larger *gem*-dialkyl groups twists the 6-membered chelate ring instead of solely compressing the β bond angle. This results in a distortion of the initial chair conformation seen for R = H, Me towards a half-boat (R = Et, *i*Pr/*i*Pent) and ultimately to a twist-boat conformation for R = *i*Pr and ^{t}Bu, as illustrated in Figure 9. These calculations were performed at 298.15 K and calculations at elevated temperature (423.15 K) have shown very similar distortions (see Figure S52).

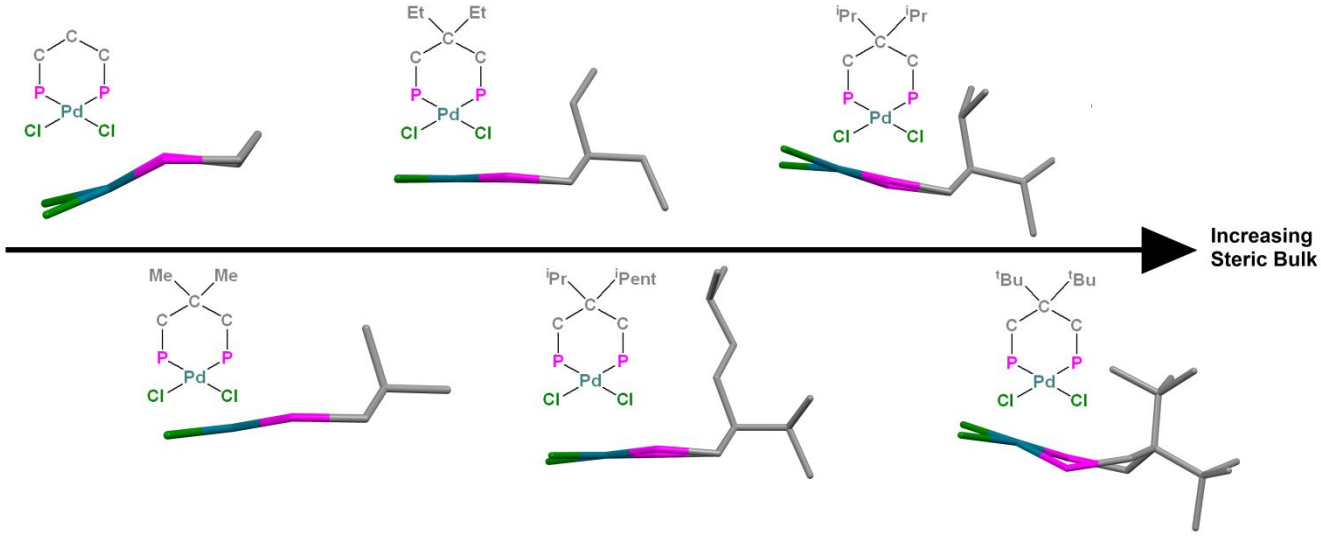

Figure 9. [Pd(**L**)Cl_2] structures calculated at room temperature and arranged by increasing steric bulk of *gem*-dialkyl substituents showing 6-member chelate conformations (side view across P–C bonds). Phenyl groups and hydrogen atoms removed for clarity.

The calculated P-Pd-P ligand bite angles follow closely the experimentally determined angles based on XRD data, reaching a maximum at 97° for R = Me and Et. For these smaller R groups (R = Me, Et), the *gem*-dialkyl effect alters the spatial environment by introducing steric bulk to the C_3-bridge that prompts a rearrangement of the phosphorus substituents (see Figure 7) and widens the ligand bite angle. For larger R groups (R = *i*Pr, ^{t}Bu), there is an accompanying distortion in the 6-membered chelate ring that results in a decrease of the P-Pd-P ligand bite angle. The accumulation of these three effects: (1) R-C-R α bond angle increase, (2) C-C-C β bond angle compression and (3) twisting of the 6-membered chelate ring, complicates the relationship between the *gem*-dialkyl effect and P-Pd-P ligand bite angle, thereby making it difficult to extract clear trends between them.

However, %V_Bur calculations indicate unambiguously that there is a general trend toward greater restriction of coordination space around the Pd metal center as R group size increases.

Table 3. Pd-Catalyzed Hydroformylation of Octene.

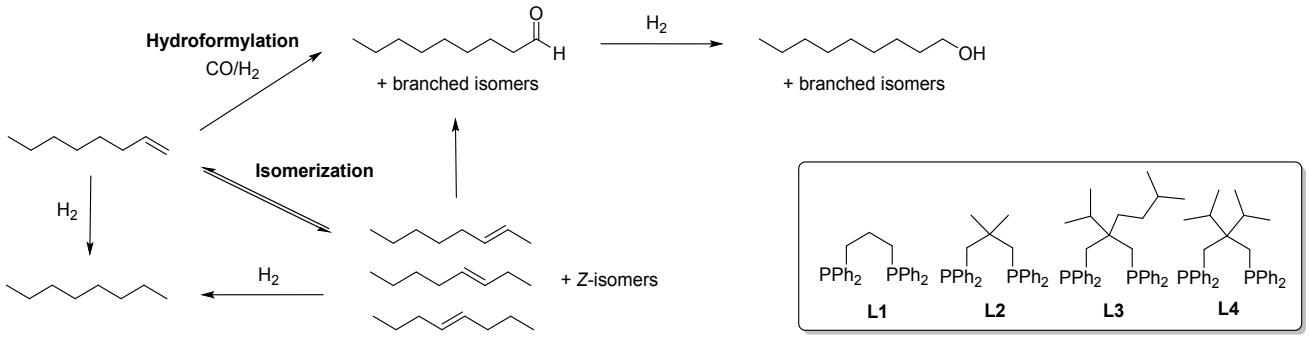

#	Olefin	L	L/ Pd	Time / h	Conv / %	Olefin Yield (Relative to All Olefins) / % 1-Oct	2-Oct	3-Oct	4-Oct	Octane	Nonanal (lin.)[a] / %	Nonanol[b] (lin.)[a] / %	Activity[c]	Mole Bal / %
1	1-octene	**L1**	2.4	5	99	1 (2)	21 (44)	17 (37)	8 (17)	4	46 (73)	2 (90)	450	99
2	1-octene	**L2**	2.4	5	99	1 (2)	26 (47)	20 (36)	8 (15)	7	36 (72)	1 (91)	450	100
3	1-octene	**L3**	2.4	5	98	2 (3)	33 (50)	22 (34)	9 (13)	8	16 (67)	6 (91)	450	96
4[d]	1-octene	**L1**	2.4	5	72	28 (44)	26 (40)	7 (11)	3 (5)	4	25 (84)	0 (n.a.)	400	93
5[d]	1-octene	**L2**	2.4	5	84	16 (26)	28 (44)	5 (8)	14 (22)	5	24 (84)	0 (n.a.)	450	92
6	1-octene	**L1**	1.1	5	99	1 (2)	23 (46)	18 (35)	9 (17)	6	42 (72)	1 (91)	450	99
7	1-octene	**L3**	1.1	5	97	3 (4)	38 (53)	23 (32)	8 (11)	9	18 (70)	2 (94)	450	100
8	1-octene	**L1**	1.1	24	99	1 (2)	10 (37)	12 (42)	5 (19)	0	67 (70)	2 (88)	600	97
9	1-octene	**L2**	1.1	24	99	1 (2)	16 (40)	17 (41)	7 (17)	0	51 (70)	2 (89)	550	94
10	1-octene	**L3**	1.1	24	99	1 (2)	21 (41)	20 (40)	9 (17)	1	34 (67)	9 (91)	550	95
11	1-octene	**L4**	1.1	24	99	1 (2)	22 (41)	22 (41)	8 (16)	0	30 (67)	9 (90)	550	92
12	*trans*-2-octene	**L1**	2.4	5	37	1 (1)	63 (81)	10 (13)	4 (5)	4	18 (71)	<1 (n.d.)	200	100
13	*trans*-2-octene	**L2**	2.4	5	27	1 (1)	73 (85)	9 (10)	3 (4)	4	7 (69)	<1 (n.d.)	100	97
14	*trans*-4-octene	**L1**	1.1	24	58	1 (1)	11 (17)	12 (18)	42 (64)	0	27 (66)	1 (83)	300	94
15	*trans*-4-octene	**L2**	1.1	24	48	1 (1)	11 (15)	11 (15)	52 (69)	0	14 (65)	1 (82)	250	90

Thermodynamic Distribution of Octene Isomers[41]	**1**	**39**	**33**	**27**

Conditions: Olefin, ligand, $Pd(OAc)_2$ (0.17 mol%), CF_3CO_2H (Acid/Pd = 50), 60 bar CO/H_2 (1:1), diglyme (0.9 M), 125 °C. Yields were determined via gas chromatography using anisole as an internal standard. Statistical error analysis based on triplicate runs: ± 3%. n.d. = not determined. n.a. = not applicable. [a] Linearity = 1-isomer / sum of all regioisomers. [b] Derivatives of alcohol products (i.e. esters/ethers) included. [c] Activity = moles of isomerization and carbonylation products / moles of catalyst. [d] Acid/Pd = 5. Note: In all runs minor amounts (<1%) of by-products such as C_{17} ketones and diglyme-derived esters were detected.

Pd-catalyzed Hydroformylation

The bidentate bis(diphenylphosphine)propane ligands **L1**-**L4** were evaluated in Pd-catalyzed hydroformylation of 1-octene and the results have been summarized in Table 3. The catalyst was formed *in-situ* by mixing $Pd(OAc)_2$ with ligand in diglyme followed by addition of CF_3COOH (see experimental section for details). The reaction conditions were based on a previous study by Drent and Budzelaar.[42-43]

Initial hydroformylation experiments of 1-octene were carried out over 5 hours with a L/Pd ratio of 2.4 and 50 equiv. CF_3COOH as a co-catalyst. The product spectrum consists of octane, a mixture of linear octenes, a mixture of linear and branched nonanal isomers, as well as some linear and branched nonanol isomers. Comparing **L1**-**L3**, while conversions are all high (>98%), a decrease in the formation of nonanal and a greater proportion of internal olefins was observed (runs 1-3). The increase in steric bulk at the ligand backbone appears to reduce the rate of hydroformylation. The ratio of linear versus branched hydroformylation products is hardly affected by the different ligands. The composition of the olefin mixture is close to the expected thermodynamic composition in all cases (1:39:33:27 for 1-, 2-, 3- and 4-octene at room temperature).[41] This indicates that the rate of isomerization must be fast in all cases relative to the rate of hydroformylation. In the case of **L3**, more hydrogenation to nonanol is observed. The lower hydroformylation activity for **L3** suggests that reductive hydroformylation from 1-octene to 1-nonanol can be favored by increasing the *gem*-dialkyl effect. The alcohol linearity is generally higher than aldehyde linearity, indicating that the hydrogenation step favors primary over secondary aldehyde substrates. A mechanism for the homogeneously catalyzed reduction of aldehydes to alcohols has been proposed by Zhou and co-workers.[44]

Lowering the amount of acid to 5 equiv. CF_3COOH results in lower conversions and less isomerization to internal olefins (runs 4-5). Isolation of the spent catalyst after the hydroformylation reaction revealed the formation of a bis(ligand) complex $[Pd(\mathbf{L1})_2](CF_3COO)_2$ (see Supporting Information). The formation of bis(ligand) complexes could be a potential catalyst deactivation pathway. However, lowering the L/Pd ratio to 1.1 gave very similar performance for ligands **L1** and **L3** (cf. run 6 vs. 1 and run 7 vs. 3), and subsequent runs were therefore carried out using this lower ratio. Extending the reaction time from 5 to 24 hours results in increased hydroformylation yields (runs 8-11), though the percentage increase is limited considering the much longer reaction time. Monitoring reactor pressures showed that the rate of syngas uptake decreases over time as expected, and that most syngas uptake occurs during the first 5 hours (see Figure 10). Initial rates determined from these curves gave a relative order for the four ligands **L1**-**L4** of 2.5: 2.0: 1.6: 1.0.

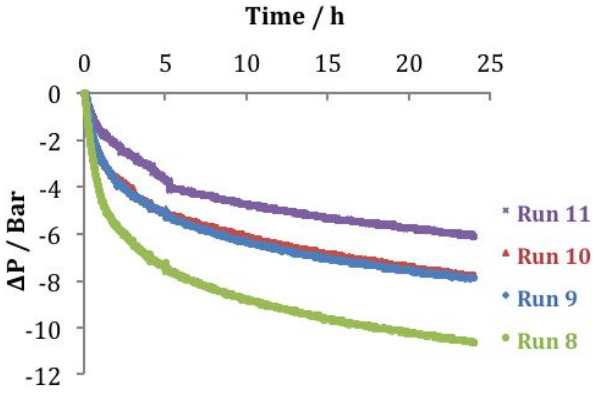

Figure 10. Pressure profile for hydroformylation runs 8-11.

After a reaction time of 24 hours, similar trends as before are seen in going from **L1**-**L4**: increasing steric bulk in the ligand backbone reduces nonanal formation, and reductive hydroformylation to alcohols increases for the bulkier ligands **L3** and **L4**. Internal alkenes (*trans*-2-octene and *trans*-4-octene) were also investigated as substrates using **L1** and **L2**. Both substrates can be hydroformylated, indicating that isomerizing hydroformylation is indeed possible with these ligands, albeit with lower conversion compared to 1-octene (runs 12-15). Hydroformylation of internal alkenes will be inherently slower than terminal alkenes, as the linear aldehyde remains the major product irrespective of the octene isomer that is used as the substrate. Isomerization from the internal octenes to 1-octene will need to occur prior to hydroformylation,[45-46] which seems to be equally fast for both ligands according to the olefin composition. The subsequent hydroformylation of 1-octene is faster for **L1** than for **L2**, as seen in runs 1-2.

The mechanism for the palladium-catalysed hydroformylation reaction has been little studied, in contrast to rhodium-catalysed hydroformylation.[19,20] Based on the currently available information, the formation of $[Pd(L)(CO)H]^+$ under the reaction conditions ($p(CO/H_2)$ = 60 bar) is assumed as the starting point in the catalytic cycle, formed from $[Pd(L)X_2]$ through heterolytic activation of H_2 and CO

coordination.[47,48] An associative substitution with the alkene substrate will give $[Pd(L)(alkene)H]^+$, which undergoes further insertion to a palladium alkyl complex. Preliminary DFT calculations (see Supporting Information) of these initial steps in the catalytic hydroformylation cycle for the complexes with ligands **L1**, **L2** and the ditert.-butyl ligand $\mathbf{L^{tBu}}$ have shown that the gem-dialkyl effect does not affect the overall energy barriers for alkene coordination and insertion (+25.3, +25.7 and +24.7 kcal/mol for **L1**, **L2** and $\mathbf{L^{tBu}}$ respectively. This is in agreement with the fast alkene isomerization seen with all catalysts. The resting state is most likely a palladium(II) acyl complex $[Pd(L)(acyl)(CO)]^+$, as seen in other palladium catalyzed carbonylation reactions (alternating CO-olefin copolymerization, olefin methoxycarbonylation, etc.) and the final hydrogenolysis step is presumed to be rate-determining in this case, similar to methanolysis and hydrolysis reactions in methoxy- and hydroxycarbonylation.[49-50] Further studies regarding the mechanism of Pd-cataylsed hydroformylation and the effect of gem-dialkyl substituents on the selectivity are ongoing.

3. CONCLUSION

A series of C_3-bridged diphosphine ligands with *gem*-dialkyl groups of varying steric bulk at the central carbon of the ligand backbone were synthesized. X-ray crystallographic analysis of the solid state structures of the $Pd(\mathbf{L})Cl_2$ complexes showed simultaneous R-C-R α bond angle expansion and C-C-C β bond angle compression as a results of the *gem*-dialkyl effect. These changes are accompanied by an unexpected distortion of the conformation of the 6-membered chelate ring formed between the ligand and the Pd metal center. DFT calculations on these and other *gem*-dialkyl groups have shown that α angles directly correlate with R group size but β angle compression goes to a minimum of about 107° before reverting to the ideal tetrahedral angle. Further inspection revealed that after the initial decrease in β angle, additional tension generated by further α angle perturbation is released via distortion of the 6-membered chair conformation toward a half-chair and eventually a twist-boat conformation. The compounding effects of α angle expansion, β angle compression and chelate distortion complicates the relationship between the *gem*-dialkyl effect and ligand bite angle. However, %V_Bur calculations indicate that the *gem*-dialkyl effect results in an increasingly crowded coordination sphere around the metal centre. The ligands were evaluated in Pd-catalyzed hydroformylation of 1-octene. A decrease in hydroformylation activity was observed as a result of the *gem*-dialkyl effect, but the bulkier **L3** and **L4** ligands showed a change in chemoselectivity to favor reductive hydroformylation to the alcohol product.

We have shown here that the gem-dialkyl effect in diphosphine ligands can be used as a parameter, in addition to ligand backbone size and the nature of the P-substituents, to affect catalyst performance. Further studies into this intriguing effect with other ligands applied in different catalytic processes are currently underway.

AUTHOR INFORMATION

Corresponding Author

*Email: g.britovsek@imperial.ac.uk

Notes

The authors declare no competing financial interest.

Supporting Information

Experimental details, NMR spectra, computational details, crystallographic details.

ACKNOWLEDGMENTS

We gratefully acknowledge the Agency for Science, Technology & Research (A*STAR) for the funding of this research. We would like to thank Angeline Seo for mass spectrometry and elemental analysis.

REFERENCES

1. van Leeuwen, P. W. N. M., *Homogeneous Catalysis - Understanding the Art*. Springer, Netherlands: 2004; p 408.
2. Kamer, P. C. J.; van Leeuwen, P. W. N. M., Phosphorus(III) Ligands in Homogeneous Catalysis: Design and Synthesis. Wiley: 2012.
3. Tolman, C. A., Steric Effects Of Phosphorus Ligands In Organometallic Chemistry And Homogeneous Catalysis. *Chem. Rev.* **1977,** *77*, 313-348.
4. Tolman, C. A., Electron Donor-Acceptor Properties Of Phosphorus Ligands. Substituent Additivity. *J. Am. Chem. Soc.* **1970,** *92*, 2953-2956.
5. Tolman, C. A., Phosphorus Ligand Exchange Equilibriums On Zerovalent Nickel. Dominant Role For Steric Effects. *J. Am. Chem. Soc.* **1970,** *92*, 2956-2965.
6. Freixa, Z.; van Leeuwen, P. W. N. M., Bite Angle Effects In Diphosphine Metal Catalysts: Steric Or Electronic? *Dalton Trans.* **2003**, 1890-1901.
7. Mansell, S. M., Catalytic Applications Of Small Bite-Angle Diphosphorus Ligands With Single-Atom Linkers. *Dalton Trans.* **2017,** *46*, 15157-15174.
8. Casey, C. P.; Whiteker, G., The Natural Bite Angle of Chelating Diphosphines. *Isr. J. Chem.* **1990,** *30*, 299-304.
9. Dierkes, P.; W. N. M. van Leeuwen, P., The Bite Angle Makes The Difference: A Practical Ligand Parameter For Diphosphine Ligands. *J. Chem. Soc., Dalton Trans.* **1999**, 1519-1530.
10. Birkholz, M.-N.; Freixa, Z.; van Leeuwen, P. W. N. M., Bite Angle Effects Of Diphosphines In C-C And C-X Bond Forming Cross Coupling Reactions. *Chem. Soc. Rev.* **2009,** *38*, 1099-1118.
11. Kamer, P. C. J.; van Leeuwen, P. W. N. M.; Reek, J. N. H., Wide Bite Angle Diphosphines: Xantphos Ligands in

Transition Metal Complexes and Catalysis. *Acc. Chem. Res.* **2001,** *34*, 895-904.
12. Arthur, K. L.; Wang, Q. L.; Bregel, D. M.; Smythe, N. A.; O'Neil, B. A.; Goldberg, K. I.; Moloy, K. G., The gem-Dialkyl Effect as a Test for Preliminary Diphosphine Chelate Opening in a Reductive Elimination Reaction. *Organometallics* **2005,** *24*, 4624-4628.
13. van Rijn, J. A.; Dunnen, A. d.; Bouwman, E.; Drent, E., Palladium–Diphosphine Complexes As Catalysts For Allylations With Allyl Alcohol. *J. Mol. Catal. A: Chem.* **2010,** *329*, 96-102.
14. van Rijn, J. A.; Siegler, M. A.; Spek, A. L.; Bouwman, E.; Drent, E., Ruthenium-Diphosphine-Catalyzed Allylation of Phenols: A gem-Dialkyl-Type Effect Induces High Selectivity toward O-Allylation. *Organometallics* **2009,** *28*, 7006-7014.
15. van Rijn, J. A.; Gouré, E.; Siegler, M. A.; Spek, A. L.; Drent, E.; Bouwman, E., The Intriguing Substitution Behavior Of CO With Bidentate Phosphine Ligands Induced By A Gem-Dialkyl Effect. *J. Organomet. Chem.* **2011,** *696*, 1899-1903.
16. Beesley, R. M.; Ingold, C. K.; Thorpe, J. F., CXIX.-The Formation And Stability Of Spiro-Compounds. Part I. Spiro-Compounds From Cyclohexane. *J. Chem. Soc., Trans.* **1915,** *107*, 1080-1106.
17. Ingold, C. K., CV.-The Conditions Underlying The Formation Of Unsaturated And Cyclic Compounds From Halogenated Open-Chain Derivatives. Part II. Products Derived From a-Halogenated Adipic Acids. *J. Chem. Soc.* **1921,** *119*, 951-970.
18. Jung, M. E.; Piizzi, G., gem-Disubstituent Effect: Theoretical Basis and Synthetic Applications. *Chem. Rev.* **2005,** *105*, 1735-1766.
19. Franke, R.; Selent, D.; Börner, A., Applied Hydroformylation. *Chem. Rev.* **2012,** *112*, 5675-5732.
20. Pospech, J.; Fleischer, I.; Franke, R.; Buchholz, S.; Beller, M., Alternative Metals for Homogeneous Catalyzed Hydroformylation Reactions. *Angew. Chem. Int. Ed.* **2013,** *52*, 2852-2872.
21. Torres, G. M.; Frauenlob, R.; Franke, R.; Borner, A., Production Of Alcohols Via Hydroformylation. *Catal. Sci. Technol.* **2015,** *5*, 34-54.
22. Misra, G. S.; Srivastava, S. B., Crossed Cannizzaro Reaction. II. *J. Prakt. Chem.* **1958,** *6*, 170-173.
23. Gao, Y.; Sharpless, K. B., Vicinal Diol Cyclic Sulfates. Like Epoxides Only More Reactive. *J. Am. Chem. Soc.* **1988,** *110*, 7538-7539.
24. Ozturk, T.; Saygili, N.; Ozkara, S.; Pilkington, M.; Rice, C. R.; Tranter, D. A.; Turksoy, F.; Wallis, J. D., Novel Organosulfur Donors Containing Hydroxy Functionalities: Synthesis Of Bis[2,2-Bis(Hydroxymethyl)Propane-1,3-Diyldithio]Tetrathiafulvalene And Related Materials. *J. Chem. Soc., Perkin Trans. 1* **2001,** 407-414.
25. Calvo-Flores, F. G.; García-Mendoza, P.; Hernández-Mateo, F.; Isac-García, J.; Santoyo-González, F., Applications of Cyclic Sulfates of vic-Diols: Synthesis of Episulfides, Olefins, and Thio Sugars. *J. Org. Chem.* **1997,** *62*, 3944-3961.
26. Kuchen, W.; Buchwald, H., Zur Kenntnis der Organophosphorverbindungen, II. Das Tetraphenyldiphosphin. *Chem. Ber.* **1958,** *91*, 2871-2877.
27. Eberhard, M. R. New Strategies In 9-Phosphabicyclononane Chemistry. PhD-Thesis, University of Bristol, 2001.
28. Harris, T. V.; Pretzer, W. R., Preparation Of A Novel Phosphorus-Phosphorus Bonded Diphosphine. *Inorg. Chem.* **1985,** *24*, 4437-4439.
29. Van Overschelde, M.; Vervecken, E.; Modha, S. G.; Cogen, S.; Van der Eycken, E.; Van der Eycken, J., Catalyst-Free Alcoholysis Of Phosphane-Boranes: A Smooth, Cheap, And Efficient Deprotection Procedure. *Tetrahedron* **2009,** *65*, 6410-6415.
30. Seetz, J. W. F. L.; Hartog, F. A.; Böhm, H. P.; Blomberg, C.; Akkerman, O. S.; Bickelhaupt, F., A Direct Synthesis Of 1,3-Bis(Bromomagnesio)Propane. *Tetrahedron Lett.* **1982,** *23*, 1497-1500.
31. Steffen, W. L.; Palenik, G. J., Crystal And Molecular Structures Of Dichloro[Bis(Diphenylphosphino)Methane]Palladium(II), Dichloro[Bis(Diphenylphosphino)Ethane]Palladium(II), And Dichloro[1,3-Bis(Diphenylphosphino)Propane]Palladium(II). *Inorg. Chem.* **1976,** *15*, 2432-2439.
32. Falivene, L.; Credendino, R.; Poater, A.; Petta, A.; Serra, L.; Oliva, R.; Scarano, V.; Cavallo, L., SambVca 2. A Web Tool for Analyzing Catalytic Pockets with Topographic Steric Maps. *Organometallics* **2016,** *35*, 2286-2293.
33. Frisch, M. J.; Trucks, G. W.; Schlegel, H. B.; Scuseria, G. E.; Robb, M. A.; Cheeseman, J. R.; Scalmani, G.; Barone, V.; Petersson, G. A.; Nakatsuji, H.; Li, X.; Caricato, M.; Marenich, A. V.; Bloino, J.; Janesko, B. G.; Gomperts, R.; Mennucci, B.; Hratchian, H. P.; Ortiz, J. V.; Izmaylov, A. F.; Sonnenberg, J. L.; Williams; Ding, F.; Lipparini, F.; Egidi, F.; Goings, J.; Peng, B.; Petrone, A.; Henderson, T.; Ranasinghe, D.; Zakrzewski, V. G.; Gao, J.; Rega, N.; Zheng, G.; Liang, W.; Hada, M.; Ehara, M.; Toyota, K.; Fukuda, R.; Hasegawa, J.; Ishida, M.; Nakajima, T.; Honda, Y.; Kitao, O.; Nakai, H.; Vreven, T.; Throssell, K.; Montgomery Jr., J. A.; Peralta, J. E.; Ogliaro, F.; Bearpark, M. J.; Heyd, J. J.; Brothers, E. N.; Kudin, K. N.; Staroverov, V. N.; Keith, T. A.; Kobayashi, R.; Normand, J.; Raghavachari, K.; Rendell, A. P.; Burant, J. C.; Iyengar, S. S.; Tomasi, J.; Cossi, M.; Millam, J. M.; Klene, M.; Adamo, C.; Cammi, R.; Ochterski, J. W.; Martin, R. L.; Morokuma, K.; Farkas, O.; Foresman, J. B.; Fox, D. J. *Gaussian 16 Rev. B.01*, Wallingford, CT, 2016.
34. Lee, C.; Yang, W.; Parr, R. G., Development Of The Colle-Salvetti Correlation-Energy Formula Into A Functional Of The Electron Density. *Phys. Rev. B* **1988,** *37*, 785-789.
35. Becke, A. D., Density-Functional Thermochemistry. III. The Role Of Exact Exchange. *J. Chem. Phys.* **1993,** *98*, 5648-5652.
36. Weigend, F., Accurate Coulomb-Fitting Basis Sets For H To Rn. *PCCP* **2006,** *8*, 1057-1065.

37. Weigend, F.; Ahlrichs, R., Balanced Basis Sets Of Split Valence, Triple Zeta Valence And Quadruple Zeta Valence Quality For H To Rn: Design And Assessment Of Accuracy. *PCCP* **2005,** *7*, 3297-3305.
38. Grimme, S., Density Functional Theory With London Dispersion Corrections. *Wiley Interdiscip. Rev.: Comput. Mol. Sci.* **2011,** *1*, 211-228.
39. Johnson, E. R.; Becke, A. D., A Post-Hartree-Fock Model Of Intermolecular Interactions: Inclusion Of Higher-Order Corrections. *J. Chem. Phys.* **2006,** *124*, 174104.
40. Johnson, E. R.; Becke, A. D., A Post-Hartree–Fock Model Of Intermolecular Interactions. *J. Chem. Phys.* **2005,** *123*, 024101.
41. Morrill, T. C.; D'Souza, C. A., Efficient Hydride-Assisted Isomerization of Alkenes via Rhodium Catalysis. *Organometallics* **2003,** *22*, 1626-1629.
42. Drent, E.; Budzelaar, P. H. M., The Oxo-Synthesis Catalyzed By Cationic Palladium Complexes, Selectivity Control By Neutral Ligand And Anion. *J. Organomet. Chem.* **2000,** *593–594*, 211-225.
43. Drent, E., Opportunities In Homogeneous Catalysis. *Pure Appl. Chem.* **1990**, *62*, 661-669.
44. Chen, Q.-A.; Ye, Z.-S.; Duan, Y.; Zhou, Y.-G., Homogeneous Palladium-Catalyzed Asymmetric Hydrogenation. *Chem. Soc. Rev.* **2013,** *42*, 497-511.
45. Vilches-Herrera, M.; Domke, L.; Börner, A., Isomerization–Hydroformylation Tandem Reactions. *ACS Catal.* **2014,** *4*, 1706-1724.
46. Kathe, P.; Fleischer, I., Cooperative Use of Brønsted Acids and Metal Catalysts in Tandem Isomerization Reactions of Olefins. *ChemCatChem* **2019,** *11,* 3343-3354.
47. Baya, M; Houghton, J.; Konya, D.; Champouret, Y.; Daran, J.-C.; Almeida Leñero, K.Q.; Schoon, L.; Mul, W.P.; van Oort, A.B.; Meijboom, N.; Drent, E.; Orpen, A. G.; Poli, R., Pd(I) Phosphine Carbonyl and Hydride Complexes Implicated in the Palladium-Catalyzed Oxo Process, *J. Am. Chem. Soc.* **2008,** *130*, 10612-10624.
48. Zuidema, E.; Bo, C.; van Leeuwen, P.W.N.M., Ester versus Polyketone Formation in the Palladium-Diphosphine Catalyzed Carbonylation of Ethene, *J. Am. Chem. Soc.* **2007**, *129*, 3989-4000.
49. Roesle, P.; Dürr, C.J.; Möller, H.M.; Cavallo, L.; Caporaso, L.; and Mecking, S., Mechanistic Features of Isomerizing Alkoxycarbonylation of Methyl Oleate , *J. Am. Chem. Soc.* **2012,** *134*, 17696-17703.
50. Zhao, L.; Pudasaini, B.; Genest, A.; Nobbs, J.D.; Low, C. H.; Stubbs, L.P.; van Meurs, M.; Rösch, N., Palladium-Catalyzed Hydroxycarbonylation of Pentenoic Acids. Computational and Experimental Studies on the Catalytic Selectivity, *ACS Catal.* **2017**, *7*, 7070-7080.

For Table of Contents Only